# Reports

## Holocene–Late Pleistocene Climatic Ice Core Records from Qinghai-Tibetan Plateau

L. G. THOMPSON, E. MOSLEY-THOMPSON, M. E. DAVIS, J. F. BOLZAN, J. DAI, T. YAO, N. GUNDESTRUP, X. WU, L. KLEIN, Z. XIE

**Three ice cores to bedrock from the Dunde ice cap on the north-central Qinghai-Tibetan Plateau of China provide a detailed record of Holocene and Wisconsin-Würm late glacial stage (LGS) climate changes in the subtropics. The records reveal that LGS conditions were apparently colder, wetter, and dustier than Holocene conditions. The LGS part of the cores is characterized by more negative $\delta^{18}O$ ratios, increased dust content, decreased soluble aerosol concentrations, and reduced ice crystal sizes than the Holocene part. These changes occurred rapidly ~10,000 years ago. In addition, the last 60 years were apparently one of the warmest periods in the entire record, equalling levels of the Holocene maximum between 6000 and 8000 years ago.**

THE DUNDE ICE CAP (38°06′N, 96°24′E) is located in a desert environment between the highest Chinese desert, the Qaidam Basin, to the south, and the Gobi Desert to the north (Fig. 1A). This relatively large ice cap has a summit elevation of 5325 m and total area of 60 km$^2$. The mean annual temperature is −7.3°C. The glacier is 140 m thick and the underlying bedrock topography is flat. About 0.4 m of water equivalent per year accumulates on the ice cap, and the firn-ice transition occurs at a depth of ~25 m (*1, 2*).

Detailed meteorological and climatological data for major parts of the Qinghai-Tibetan Plateau, including the surrounding mountains, are lacking (*3*). Ice core records from selected ice caps on the plateau that can be highly resolved in time and that contain Holocene to Late Pleistocene ice would allow development of a spatially coherent climate history. Such records would greatly enhance our understanding of the global climate system because of the significance of this region for affecting large-scale climate.

In 1987, three ice cores were recovered to bedrock from the Dunde ice cap summit (Fig. 1): cores D-1 (139.8 m), D-2 (136.6 m), and D-3 (138.4 m). The visible stratigraphy of each core was photographically recorded immediately after drilling. Core D-1 was then cut into 3585 samples that were melted in closed containers by passive solar heating in a laboratory tent. Samples were divided so that microparticle concentrations (MPC) and O isotopic ratios ($\delta^{18}O$) could be measured on the same sample. The upper 56 m of core D-3 were melted and bottled on site while the lower 83 m were kept frozen. The concentrations of $NO_3^-$, $SO_4^{2-}$, $Cl^-$, and *p*H were measured for the entire length of D-3, and crystal sizes and cations were measured for selected sections (*4–6*).

Surface and basal borehole temperatures were −7.3°C and −4.7°C, respectively. At the summit of the ice cap, ice layers can form during the summer as a result of the intense radiation. Summer melt, as shown by ice layers in the firn, generally makes up less than 5% of the annual precipitation (*2*).

The MPC and O isotope stratigraphy show an annual variation (*2*) that is discernible down to about 70 m depth. Below this level, the sampling interval (3 cm) was too large to enable resolution of the annual signal. However, enhanced dust deposition during the dry season produced stratigraphic markers that are visible deeper in the ice. These were used to identify annual layers to about 117 m depth (Fig. 2). Counting the annual $\delta^{18}O$ and MPC peaks to 70 m and the visible dust layers below 70 m indicates that the ice at 117 m depth was deposited about 4550 years ago.

The age of the deeper ice can be roughly estimated by extrapolation of the annual layer thickness data. The D-1 borehole was located close to the flow divide or center of flow. A variety of data (*7–9*) suggest that ice deformation as a function of depth is different near a flow divide than at distances many ice thicknesses away. Although derived from a deep temperature profile from the Dome C ice divide in East Antarctica (*8*), the following analytical expression provides a good representation of the annual layer thickness data in the D-1 core

$$L(z) = b(1 - z/H)^{p+1} \quad (1)$$

where $z$ and $H$ are the ice-equivalent depth and thickness, respectively, and $b$ is the average annual accumulation rate (meters per year) over the depth interval of interest; $p$ is a constant to be determined.

Measurements of gross beta radioactivity from the 1987 D-1 and D-3 cores allowed identification of the 1963 atmospheric nuclear testing horizon; the calculated average accumulation rate between 1963 and 1987

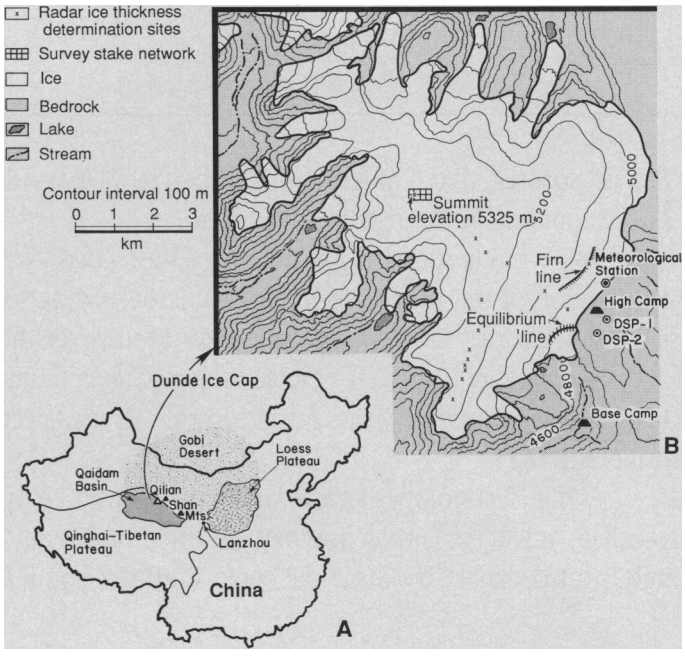


**Fig. 1.** (**A**) Location of the Dunde ice cap, Qaidam Basin, and Loess Plateau and (**B**) topography of the ice cap, position of the survey network, firn and equilibrium lines, and sites where ice thickness was determined.

L. G. Thompson, E. Mosley-Thompson, M. E. Davis, J. F. Bolzan, J. Dai, L. Klein, Byrd Polar Research Center, Ohio State University, Columbus, OH 43210.
T. Yao, X. Wu, Z. Xie, Lanzhou Institute of Glaciology and Geocryology, Academic Sinica, Lanzhou, China.
N. Gundestrup, Isotope Laboratory, Geophysical Institute, University of Copenhagen, Denmark.

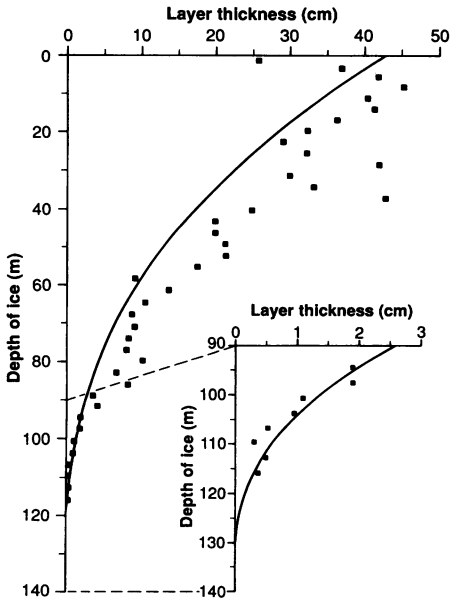


**Fig. 2.** Average annual layer thicknesses (■) based upon the visible dust layers as a function of depth in core D-1. The inset shows the thicknesses in detail from 90 m to the bottom of the core. The curve represents the calculated variation of layer thickness with depth from Eq. 1 with the parameters $p = 1.612$ and $b = 0.428$ m per year.

was about 0.42 m/year (ice equivalent). The average measured value from 31 stakes in the summit strain network for the 1986–1987 accumulation year was 0.37 m (ice equivalent). If the 24-year average value is assumed to be characteristic of the Holocene, the exponent $p$ is fixed by the requirement that the ice at 117 m depth was deposited 4550 years ago. The age at the prominent stratigraphic transition (Fig. 3) at 129.2 m depth in the D-1 core (125.8-m ice equivalent) is then calculated to be about 11,950 years ago. In consideration of the uncertainty in the accumulation rate assumption, this age is close to the annually dated age of 10,750 years ago for the LGS-Holocene transition in the Camp Century core from northern Greenland (*10*).

We estimated the age near the bottom of the D-1 core (Figs. 3 and 4) by fixing the age at the LGS-Holocene transition at 10,750 years ago and using the dated horizon at 117 m depth. Although these results are rough because pronounced variations in accumulation rate and shape of the ice sheet no doubt have occurred over long periods of time, these estimates suggest that the record is potentially more than 100,000 years old.

All major dust events in the glacial stage ice of core D-1 also occur in core D-3. These data indicate that the records are continuous through the lowest sections of both cores. As is the case for the relatively shallow ice caps in the Canadian arctic islands (*11, 12*), the high-altitude, subtropical ice caps of the Qinghai-Tibetan Plateau can provide climatic records comparable in length with those obtained in Greenland and Antarctica, although the oldest sections of the record are much more compressed.

Late in the 1986 field season, an abrupt contact was observed between clean ice and underlying dirty ice emerging along the margin of the Dunde ice cap. The MPC and $\delta^{18}O$ analyses of two shallow cores drilled through this transition indicated that the underlying ice was probably of Wisconsin-Würm LGS age (*1*). In core D-1 at the summit there is also a large increase in dust and $\delta^{18}O$ depletion (Fig. 3) at 129.2 m; the MPCs increase substantially over the Holocene average. The increase in dust and decrease in the $^{18}O/^{16}O$ ratio are also observed in LGS ice from polar cores. In cores from Camp Century (*5*) and Dye 3 (*13*) in Greenland, the transition from high dust concentrations in LGS ice to low concentrations in Holocene ice is also abrupt. In the Dunde ice cores, the transition in the dust concentration is completed within a 30-cm section of ice representing approximately 40 years.

The more negative $\delta^{18}O$ ratios in the lower 10 m of D-1 are consistent and strongly support the interpretation that LGS ice is present, even though the mean change in $\delta^{18}O$ of 2 per mil is substantially less than the change of 11 per mil at Camp Century, 8 per mil at Devon Island, and 5 to 7 per mil in Antarctica (*13–15*). This small change in the D-1 core implies that the temperature decrease during the glacial stage on the subtropical Qinghai-Tibetan Plateau was less than in the polar regions. Because more than 85% of the annual snowfall on the Dunde ice cap arrives during the monsoon season (June through August), the isotope record is mainly a proxy of summer temperature. A moderate temperature decrease during the LGS at lower latitudes is consistent with the 1981 CLIMAP (*16*) sea-surface temperature reconstructions for approximately 18,000 years ago. A variety of data suggests that large areas of the tropics and subtropics had sea-surface temperatures as warm as or slightly warmer than those today. Moreover, the O isotope record in the Dunde ice cores was not affected by variations in sea ice cover during glacial stages. In the polar regions, such changes can increase the distance to moisture sources, which will tend to reduce $^{18}O/^{16}O$ ratios in ice core records during colder climates. Unlike the rapid transition in MPC and anion concentrations at the LGS-Holo-

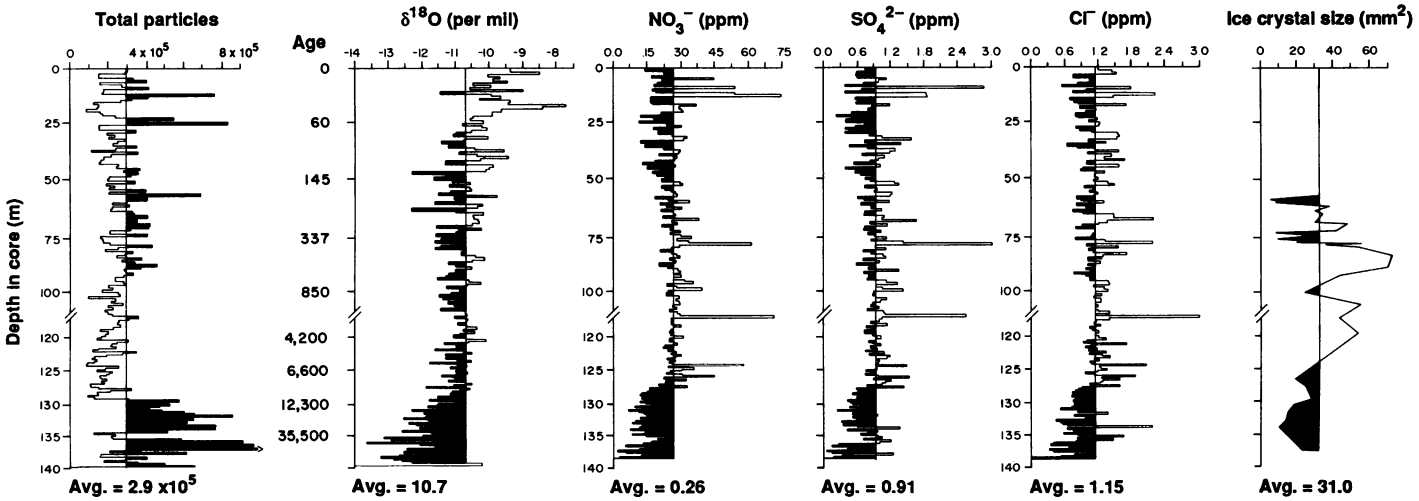


**Fig. 3.** Averages over 1-m depth intervals (0 to 120 m) and 0.5-m depth intervals (120 to 139.8 m) for total particles (diameters ≥2.0 μm) per milliliter of sample and $\delta^{18}O$ in core D-1 and $NO_3^-$, $SO_4^{2-}$, and $Cl^-$ in core D-3. The particle and $\delta^{18}O$ profiles are based on analysis of 3585 samples, the chemistry profiles are derived from analysis of 1200 individual samples, and the ice crystal sizes are measurements on 33 selected sections of core below 50 m; avg, average; age is in years ago.

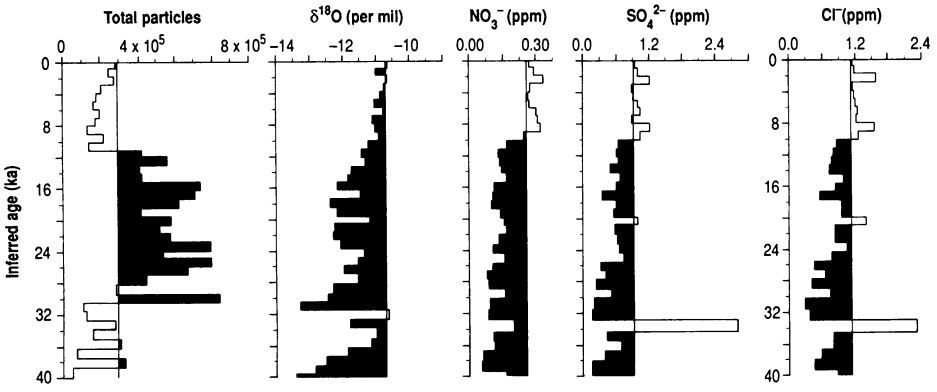


**Fig. 4.** Discrete 1,000-year averages of dust concentrations (diameters ≥2.0 μm) and $\delta^{18}O$ in core D-1 and $NO_3^-$, $SO_4^{2-}$, and $Cl^-$ in core D-3 for the last 40,000 years. The average values are for all samples in the 40,000-year record and not for the individual 1,000-year averages. There are 5 m of ice core below the 40,000-year model cutoff shown here; ka, thousand years ago.

cene boundary in the Dunde ice cores, the increase in $\delta^{18}O$ in precipitation appears to be more gradual, occurring over several centuries.

Concentrations of $Cl^-$, $SO_4^{2-}$, $Na^+$, $Ca^{2+}$, and $Mg^{2+}$ vary similarly throughout the cores. Alkaline cations ($Na^+$, $Ca^{2+}$, and $Mg^{2+}$) and $SO_4^{2-}$, $Cl^-$, and $HCO_3^-$ (estimated with *p*H) constitute the majority of the dissolved species in D-3. The concentrations of anion species decrease sharply in the lower 12 m of D-3 (Fig. 3), where average concentrations of $NO_3^-$, $SO_4^{2-}$, and $Cl^-$ are 30, 50, and 32% of their respective averages for the entire core. The concentrations of major cations are also lower in this part of the core. This decrease of the ionic concentrations in core D-3 is temporally correlative with the increase in microparticle concentrations below 129 m of core D-1, where there is a similarly abrupt transition. In contrast, LGS concentrations of soluble species ($SO_4^{2-}$, $Cl^-$) in polar ice cores are generally higher than those in the Holocene (*17, 18*). The decrease from LGS to Holocene concentration in the polar cores is attributed to increased precipitation and reduced long-distance transport of terrestrial dust and sea-salt aerosol during the Holocene.

Ice crystal sizes were measured for selected sections of D-3 in ice below 56 m (Fig. 3) to explore the possibility that temperature (*19*) and dust (*20*) affect size, as reported in polar ice cores. Crystal growth rate increases with temperature (*21*). Between 56 and 89 m, a growth rate of 0.2 $mm^2$ per year was calculated, which, if applied to the entire core, would imply that at 128.5 m, the crystal size would be 300 $mm^2$. However, crystal size decreased substantially in LGS ice where a minimum of 11.4 $mm^2$ was measured. Similarly, LGS ice in cores from Antarctica (*19*) and Greenland (*18*) is characterized by substantially smaller crystals.

On the basis of these data, we conclude that the lower 10 to 12 m of ice in the Dunde ice cap represent ice deposited during the last glacial stage. The high dust concentrations correlate closely with $\delta^{18}O$ depletion (temperature proxy), as in all polar cores extending below the LGS-Holocene transition; the association of high dust content and more negative $\delta^{18}O$ has been commonly considered the principal characteristic of LGS ice in polar ice cores (*11, 13, 21–26*).

The Dunde ice cores provide a record of the late glacial climatic and environmental conditions on the Qinghai-Tibetan Plateau (Fig. 4). The high alkalinity and NaCl concentrations suggest that the dust deposited on the ice cap originated from the surrounding deserts and salt deposits. The consistent ratios among major anion and cation concentrations throughout the cores suggest that the provenance of the dust has not changed much over the last ~40,000 years. The reduced concentrations of dissolved species in LGS ice may reflect higher precipitation rates during LGS than in the Holocene. A large part of the Qaidam Basin was apparently covered by freshwater lakes during the LGS (*27*). Dessication of the lakes began in the latter part of the LGS in response to reduced precipitation or reduced precipitation to evaporation ratios, and extensive evaporite deposits were formed. As the Holocene is approached, the increasing ion concentrations probably reflect both decreased precipitation and increased dry surface area in the Qaidam Basin.

Enhanced dust deposition in LGS ice may have resulted from increased wind strength in response to increased baroclinicity (steeper isobaric and isothermic gradients) (*28, 29*) around the expanded continental ice sheet in the higher latitudes. During the LGS, high winds from the deserts of western Asia deposited loess hundreds of feet thick across central and eastern China; similar deposits extend to the Pacific Basin (*30*) and most likely to North America. Large dust events must have occurred over the Dunde ice cap and most likely much of the extensively snow-covered and glaciated plateau. The rapid decrease in dust deposition at the LGS-Holocene transition (~40 years) could reflect substantial change in the prevailing climatic conditions that limited the capability of the atmosphere to transport dust.

The $\delta^{18}O$ record (Fig. 4) reveals a short interval of apparent warming about 35,000 years ago that is also associated with less dust deposition. Full glacial conditions were soon reestablished. Between 30,000 and 10,000 years ago, concentrations of $Cl^-$ and $SO_4^{2-}$ increased gradually. One explanation for this increase is that conditions became drier and the areal extent of salt and loess deposits increased. About 10,750 years ago, a marked increase occurred, probably reflecting the drying of the freshwater lakes. Simultaneously, the insoluble dust decreased sharply (Figs. 3 and 4). The $\delta^{18}O$ profile suggests that there was a gradual warming at the boundary while the aerosol (soluble and insoluble) data suggest that other environmental changes, including reduced deposition, were rapid as might be produced by a reduction in wind intensity.

A striking feature of the $\delta^{18}O$ record (Fig. 3) is the extreme less negative values (which suggest warmer temperatures) of the last 60 years; decades with the highest values are the 1940s, 1950s, and 1980s. The only comparable values are for the Holocene maximum, 6000 to 8000 years ago. Climate model results of Hansen and others (*31*) suggest that the central part of the Asian continent might be strongly affected by the anticipated greenhouse warming. Although the Dunde ice core (D-1) data suggest that the recent warming on the Tibetan Plateau has been substantial, a connection with the greenhouse warming has not been established.



## REFERENCES AND NOTES

1. L. G. Thompson, E. Mosley-Thompson, X. Wu, Z. Xie, *Geojournal* **174**, 517 (1988).
2. L. G. Thompson, X. Wu, E. Mosley-Thompson, Z. Xie, *Ann. Glaciol.* **10**, 178 (1988).
3. M. Domrös and G. Peng, *The Climate of China* (Springer-Verlag, Berlin, 1988).
4. Core D-1 was analyzed at both the Byrd Polar Research Center (BPRC) and the Lanzhou Institute of Glaciology and Geocryology (LIGG), core D-2 at LIGG, and core D-3 at BPRC; $\delta^{18}O$ was measured at the University of Copenhagen and all other measurements were made at BPRC under class 100 clean room conditions. The concentrations of particles with diameters ≥2.0 μm per milliliter of sample (MPC) were measured with model TA-II Coulter Counters (*5*). The high concentrations of dust necessitated diluting most of the samples 36 times (up to 7000 times in extreme cases) to avoid problems with coincident passage through the aperture tube. Samples for chemistry and $\delta^{18}O$ were not diluted. The

concentrations of seven major ions, $Cl^-$, $SO_4^{2-}$, $NO_3^-$, $Na^+$, $K^+$, $Mg^{2+}$, $Ca^{2+}$, were measured with a Dionex Model 2010i chromatograph, equipped wth AS4A (for anions) and FAST SEP CATION I and II (for cations) columns. Samples of 200 to 250 g were cut from both D-1 and D-3 and pumped through ion-exchange filters to measure total beta radioactivity in a Tennelec LB 1000 series Alpha/Beta Counting System. Total beta radioactivity is routinely used to identify time-stratigraphic horizons associated with known atmospheric thermonuclear tests (*6*).
5. L. G. Thompson, *Microparticles, Ice Sheets and Climate* [*Rep. 64*, Institute of Polar Studies (now Byrd Polar Research Center) Ohio State University, Columbus, OH, 1977].
6. G. Crozaz, C. C. Langway, Jr., E. Picciotto, *U.S. Army Corps Eng. Cold Reg. Res. Eng. Lab. Res. Rep. 208* (1966).
7. C. F. Raymond, *J. Glaciol.* **29**, 357 (1983).
8. J. F. Bolzan, *J. Geophys. Res.* **90**, 8111 (1985).
9. N. Reeh, *J. Glaciol.* **34**, 46 (1988).
10. C. U. Hammer, H. B. Clausen, H. Tauber, *Radiocarbon* **28**, 284 (1988).
11. D. A. Fisher *et al.*, *Nature* **301**, 205 (1983).
12. W. S. B. Paterson *et al.*, *ibid.* **266**, 508 (1977); R. M. Koerner, *IAHS AISH Publ. 118* (1977), p. 371.
13. C. U. Hammer *et al.*, in *Greenland Ice Core: Geophysics, Geochemistry, and the Environment*, C. C. Langway, Jr., H. Oeschger, W. Dansgaard, Eds. (*Geophys. Monogr. 33*, American Geophysical Union, Washington, DC, 1985), pp. 90–94.
14. S. J. Johnsen, W. Dansgaard, H. B. Clausen, C. C. Langway, Jr. *Nature* **235**, 429 (1972).
15. C. Lorius, L. Merlivat, J. Jouzel, M. Pourchet, *ibid.* **280**, 644 (1979).
16. CLIMAP Project Members, *Geol. Soc. Am. Map Chart Ser. MC-36* (1981).
17. M. R. Legrand and R. J. Delmas, *Ann. Glaciol.* **10**, 116 (1988).
18. S. L. Herron and C. C. Langway, Jr., in *Greenland Ice Core: Geophysics, Geochemistry, and the Environment*, C. C. Langway, Jr., H. Oeschger, W. Dansgaard, Eds. (*Geophys. Monogr. 33*, American Geophysical Union, Washington, DC, 1985), pp. 77–84.
19. J. R. Petit, P. Duval, C. Lorius, *Nature* **326**, 62 (1987).
20. R. M. Koerner and D. Fisher, *J. Glaciol.* **89**, 209 (1979).
21. P. Duval and C. Lorius, *Earth Planet Sci. Lett.* **48**, 59 (1980).
22. L. G. Thompson and E. Mosley-Thompson, *Science* **212**, 812 (1981).
23. W. Dansgaard, H. B. Clausen, N. Gundestrup, S. Johnsen, C. Rygner, in *Greenland Ice Core: Geophysics, Geochemistry, and the Environment*, C. C. Langway, Jr., H. Oeschger, W. Dansgaard, Eds. (*Geophys. Monogr. 33*, American Geophysical Union, Washington, DC, 1985), pp. 71–76.
24. R. M. Koerner, D. A. Fisher, W. S. B. Paterson, *Can. J. Earth Sci.* **24**, 296 (1987).
25. M. DeAngelis, N. I. Barkov, V. N. Petrov, *Nature* **325**, 318 (1987).
26. L. G. Thompson, E. Mosley-Thompson, J. R. Petit, *Sea Level, Ice, and Climate Change* (International Association of Hydrological Sciences, Canberra, Australia, 1979), pp. 227–234.
27. K. Chen and J. M. Bowler, *Palaeogeogr. Palaeoclimatol. Palaeoecol.* **54**, 87 (1985).
28. S. Manabe and D. G. Hahn, *J. Geophys. Res.* **82**, 3889 (1977).
29. W. L. Gates, *Science* **191**, 1138 (1976).
30. D. K. Rea, M. Lewen, T. R. Janecek, *ibid.* **227**, 4688 (1985).
31. J. Hansen *et al.*, *J. Geophys. Res.* **93**, 9341 (1988).
32. Supported by the National Science Foundation Office of Climate Dynamics and the Division of Polar Programs (ATM-8519794), the National Geographic Society (3323-86), the Ohio State University and Academia Sinica of China. We thank the many individuals who contributed to the success of this program, especially the 50 Chinese and American participants. Initial support was provided by the National Academy of Sciences' Committee for Scholarly Communication with the People's Republic of China. We thank B. Koci and the Polar Ice Coring Office for drilling the cores, the F. C. Hansen Company for assistance in the modification of a tree-ring incremental measuring device for use in ice core dating, S. Smith for illustrations, and K. Doddroe for typing. This paper is Contribution 655 of the Byrd Polar Research Center, The Ohio State University.

16 June 1989; accepted 23 August 1989

# Carbon Dioxide Transport by Ocean Currents at 25°N Latitude in the Atlantic Ocean

PETER G. BREWER, CATHERINE GOYET, DAVID DYRSSEN

**Measured concentrations of $CO_2$, $O_2$, and related chemical species in a section across the Florida Straits and in the open Atlantic Ocean at approximately 25°N, have been combined with estimates of oceanic mass transport to estimate both the gross transport of $CO_2$ by the ocean at this latitude and the net $CO_2$ flux from exchange with the atmosphere. The northward flux was $63.9 \times 10^6$ moles per second (mol/s); the southward flux was $64.6 \times 10^6$ mol/s. These values yield a net $CO_2$ flux of $0.7 \times 10^6$ mol/s (0.26 ± 0.03 gigaton of C per year) southward. The North Atlantic Ocean has been considered to be a strong sink for atmospheric $CO_2$, yet these results show that the net flux in 1988 across 25°N was small. For $O_2$ the equivalent signal is $4.89 \times 10^6$ mol/s northward and $6.97 \times 10^6$ mol/s southward, and the net transport is $2.08 \times 10^6$ mol/s or three times the net $CO_2$ flux. These data suggest that the North Atlantic Ocean is today a relatively small sink for atmospheric $CO_2$, in spite of its large heat loss, but a larger sink for $O_2$ because of the additive effects of chemical and thermal pumping on the $CO_2$ cycle but their near equal and opposite effects on the $CO_2$ cycle.**

THE NORTH ATLANTIC OCEAN HAS been widely regarded as an important $CO_2$ sink and heat source for the atmosphere. The large-scale circulation consists of both the horizontal wind-driven gyre circulation and the vertically overturning thermohaline-driven circulation. Both act in concert to transport heat and trace greenhouse gases to latitudes where disequilibrium with the atmosphere occurs. Linkage of the heat and gas fluxes is a necessary component of carbon cycle and climate modeling, yet calculations of these fluxes have proceeded along independent paths. We have measured oceanic $CO_2$ concentrations and related chemical properties (temperature, salinity, $O_2$ and $NO_3$ concentrations, and alkalinity) in a section through the Florida Straits at 26.5°N (Hollywood, Florida, to Great Isaacs Rock, Bahamas) and in the open Atlantic Ocean at 25°N (Bahamas to Africa) in order to test an earlier and controversial hypothesis of Brewer and Dyrssen (*1*), based on a few data, that treatment of $CO_2$ data in a manner identical to that used for heat transport would yield a very small net $CO_2$ flux.

The section is the same as that used by others for the estimate of heat flux (*2*), and we made specific use of the oceanic transports of water derived from these studies to compute the chemical fluxes. The work was carried out on the Research Vessel *Oceanus* Cruise 205 in November 1988 at five stations across the Florida Straits and four stations in the open Atlantic (Fig. 1). Time did not permit a full oceanic section, and thus interpolation along density surfaces sampled by others (*2–4*) was necessary.

For the North Atlantic, the earlier calculations (*2–4*) have shown that the northward flow of 30 Sverdrups (Sv) (*5*), principally through the Florida Straits, has a mean temperature of 18.8°C, and that the compensating return flow has a mean temperature of 9.7°C. This difference provides the observed net heat flux of $\sim 1.1 \times 10^{15}$ W. Although some uncertainty still surrounds this estimate (*6*), on the basis of atmospheric observations, the oceanic data are compelling.

The equivalent calculation for trace gases is more difficult because of the technical difficulty of obtaining measurements and the enrichment of gases in the cold, deep flows where mass transports are less easily determined. Moreover heat is an internally conserved property of sea water, whereas the biogenic gases are transferred both at the sea surface, because of thermal, partial pressure, and biogenic processes, and internally,

P. G. Brewer and C. Goyet, Department of Chemistry, Woods Hole Oceanographic Institution, Woods Hole, MA 02543.
D. Dyrssen, Department of Analytical and Marine Chemistry, Chalmers University of Technology, S-412 96 Göteborg, Sweden.